# Critical behavior of a one-dimensional fixed-energy stochastic sandpile

Ronald Dickman<sup>1</sup>, Mikko Alava<sup>2</sup>, Miguel A. Muñoz<sup>3</sup>, Jarkko Peltola<sup>2</sup>, Alessandro Vespignani<sup>4</sup>, and Stefano Zapperi<sup>5</sup>

<sup>1</sup> Departamento de Física, ICEx, Universidade Federal de Minas Gerais, Caixa Postal 702, 30161-970 Belo Horizonte, MG, Brazil

<sup>2</sup> Helsinki University of Technology, Laboratory of Physics, HUT-02105 Finland

<sup>3</sup> Institute Carlos I for Theoretical and Computational Physics

and Departamento de Electromagnetismo y Física de la Materia

18071 Granada, Spain.

<sup>4</sup> The Abdus Salam International Centre for Theoretical Physics (ICTP) P.O. Box 586, 34100 Trieste, Italy

<sup>5</sup> INFM, Dipartimento di Fisica, E. Fermi, Universitá de Roma "La Sapienza", P.le A. Moro 2, 00185 Roma, Italy

(March 22, 2022)

# Abstract

We study a one-dimensional fixed-energy version (that is, with no input or loss of particles), of Manna's stochastic sandpile model. The system has a continuous transition to an absorbing state at a critical value  $\zeta_c$  of the particle density. Critical exponents are obtained from extensive simulations, which treat both stationary and transient properties. In contrast with other one-dimensional sandpiles, the model appears to exhibit finite-size scaling, though anomalies exist in the scaling of relaxation times and in the approach to the stationary state. The latter appear to depend strongly on the nature of the initial configuration. The critical exponents differ from those expected at a linear interface depinning transition in a medium with point disorder, and from those of directed percolation.

Typeset using  $\text{REVT}_{EX}$ 

## I. INTRODUCTION

Sandpile models are the prime example of self-organized criticality (SOC), or scaleinvariance in the apparent absence of tuning parameters [1–4]. SOC in a slowly driven sandpile has an analog in the absorbing-state phase transition of the corresponding nondriven or fixed-energy sandpile (FES) [3–8]. While most studies of sandpiles have probed the slowdriving limit (addition and loss of sand grains at an infinitesimal rate), there is great interest in understanding the scaling properties of FES models as well [7,9–11]. One may hope that these systems, which are isolated and translation-invariant, will prove easier to characterize than driven sandpiles, which have eluded a rather massive theoretical and computational effort to obtain precise critical exponents or assign universality classes. In this paper we present extensive numerical results for a particularly simple one-dimensional FES. Analogous studies of higher dimensional systems can be found in [7,8,12] (A review of these results and related models can be found in Refs. [3,4]).

One of the central features of sandpile models is the presence of a conserved field, which may be thought of as the density of sand grains, or, in our nomenclature, the energy density. This field is conserved locally as well as globally, and couples to the activity density, which is the order parameter. The configuration evolves through a series of "toppling" events, i.e., redistributions of energy from an active site to its neighbors, which may be either deterministic or stochastic. The well known Bak-Tang-Wiesenfeld (BTW) sandpile has a deterministic toppling rule, and is also Abelian (the final absorbing configuration is independent of the order of toppling), which allows many stationary-state properties of the driven sandpile to be found exactly [13,14]. A less desirable aspect of the deterministic dynamics, on the other hand, is that in the steady-state only a small subset of the possible configurations (determined by the initial state) are visited [13]. This leads to strong nonergodic effects in the FES version of the BTW automaton [12]. Here we study a one-dimensional stochastic FES sandpile to elucidate the consequences of stochastic rules.

In our model, a variant of the Manna sandpile [15,16], the pair of particles liberated when a site topples move *independently*, and with equal probability, to the nearest neighbors on the left or right. We may therefore think of the particles as independent random walkers. (There is no restriction on the number of walkers at a given site.) While the walkers are independent as far as their hopping direction is concerned, their mobility does involve an interaction: isolated particles cannot move, but if two or more particles occupy the same site, the site may topple. Thus for densities  $\zeta = N/L \leq 1$  (N is the number of walkers on a ring of L sites), absorbing configurations exist, in which all walkers are paralyzed. But since the fraction of absorbing configurations vanishes as  $\zeta \to 1$ , it is reasonable to expect a phase transition from an absorbing to an active phase at some  $\zeta_c < 1$ . Simulations bear this out, and show that there is a continuous transition at  $\zeta_c \simeq 0.9488$ .

Our goal in the present paper is to determine the critical behavior of the model. To this end, we analyze the static behavior and the approach to the steady state in the language of absorbing-state phase transitions, studying the order parameter, its fluctuations, and temporal correlations. We also investigate the cumulative local activity, whose dynamics obeys a linear diffusion equation in the presence of an effective quenched noise term that reflects the stochastic redistribution rules, the Linear Interface Model (LIM) [17–20]. Our main finding is that the one-dimensional Manna model defines a universality class different both from that of directed percolation, and of the linear interface model. The existence of long-range correlations that arise from a conservation law is believed to be at the basis of this new universality class [7,8,12,21].

The paper is structured as follows. In Sec. II we define the model and our simulation algorithm. Numerical results are analyzed, in the contexts of absorbing-state phase transitions and of driven interfaces, in Sec. III. In Sec. IV we summarize and discuss our findings.

## II. MODEL

The model is defined on a one-dimensional lattice with periodic boundaries. The configuration is specified by the energy (or number of walkers)  $z_i = 0, 1, 2, ...$  at each site; sites with  $z_i \ge 2$  are said to be *active*. A Markovian dynamics is defined by the toppling rate, which is unity for all active sites, and zero for sites with  $z_i < 2$ . When a site *i* topples,  $z_i \rightarrow z_i - 2$  and the two particles liberated move *independently* to randomly chosen nearest neighbors *j* and *j'* (*j*, *j'*  $\in \{i+1, i-1\}$ ). (Thus j = j' with probability 1/2.) In most cases we use random sequential dynamics: the next site to topple is chosen at random from a list of active sites, which must be updated following each toppling event. The time increment associated with each toppling is  $\Delta t = 1/N_A$ , where  $N_A$  is the number of active sites just prior to the toppling. In this way,  $\langle N_A \rangle$  sites on average topple per unit time, just as they would in a simultaneously updated version of the model, in which all active sites at time  $t_n$  are toppled simultaneously and  $\Delta t \equiv 1$ . We expect the two dynamics to be equivalent insofar as scaling properties are concerned, and note that the latter choice was used in some of the interface representation studies discussed below.

In most of our simulations, the initial condition is generated by distributing  $\zeta L$  particles randomly among the L sites, yielding an initial (product) distribution that is spatially homogeneous and uncorrelated. Once the particles have been placed, the dynamics begins (we verified that allowing some toppling events *during* the insertion phase has no effect on the stationary properties). The condition of having at least one active site in the initial configuration is trivially satisfied on large lattices, for the  $\zeta$  values of interest, i.e., close to the critical value. In fact, for large L, the initial height at a given site is essentially a Poisson random variable, and the probability of having no active sites decreases exponentially with the lattice size. It is worth remarking that while the initial conditions are statistically homogeneous, the energy density is not perfectly smooth. For  $1 \ll l \ll L$ , the energy density on a set of  $l^d$  sites is essentially a Gaussian random variable with mean  $\zeta$  and variance ~  $l^{-d}$ . Such initial fluctuations relax on a time scale ~  $l^{z_D}$  with  $z_D \geq 2$ . That is, the exponent governing diffusive relaxation must be at least as large as for independent random walkers. (Recall that in our model regions of lower density will exhibit less activity, hence a slower redistribution of particles.) The initial value of the critical-site density,  $\rho_c$  (the density of sites with  $z_i = 1$ ), moreover, is generally far from its stationary value, complicating relaxation to the steady state. These observations are pertinent to the studies of modified initial conditions reported in Sec. IIId.

If after some time the system falls into a configuration with no active sites, the dynamics is permanently frozen, i.e., the system has reached an absorbing configuration. We shall see that as we vary  $\zeta$ , the model exhibits a phase transition separating an absorbing phase (in which the system always falls into an absorbing configuration), from an active phase possessing sustained activity.

#### **III. SIMULATION RESULTS**

#### A. Absorbing-state phase transition

The presence of an absorbing-state phase transition is a general feature of FES models [7,8,12]. In analogy with standard analyses of such transitions, it is possible to derive a set of Langevin equations describing their critical behavior in high dimensions. Following Ref. [12], we can write the dynamical equations for the density of active sites  $\rho_a$  and the energy density  $\zeta$  as

$$\partial_t \rho_a = D\nabla^2 \rho_a + \mu \rho_a - b\rho_a^2 + w\zeta \rho_a + \rho_a^{1/2}\eta \tag{1}$$

$$\partial_t \zeta = \lambda \nabla^2 \rho_a,\tag{2}$$

where  $\mu$ , b, w and  $\lambda$  are coupling constants and  $\eta$  is a Gaussian noise. Eqs. (1-2) closely resemble the Langevin field theory of directed percolation (DP), apart from an additional coupling between the activity and the energy field, which is conserved by the dynamics. Due to this coupling, the FES critical behavior is not in the DP universality class, but belongs to a new universality class embracing all systems with multiple absorbing states in which the order parameter is coupled to a static conserved field [21,22]. (By 'static' we mean that this field is frozen in regions where the order parameter is null.) The field theory for a reactiondiffusion model in this universality class has been derived exactly; it reproduces in some limits Eqs. (1-2) [22]. It is thus interesting to study the critical behavior in d = 1, to see if it is possible to generalize the known results for fixed-energy sandpiles [12] to one-dimensional systems.

We simulated the model using system sizes ranging from L = 100 to about  $10^4$  sites. (Since  $\zeta = N/L$  with N an integer, we are obliged to use different sets of L values to study different energy densities  $\zeta$ .) In stationary-state simulations, we collect data over an interval of  $t_m$  time units, following a relaxation period of  $t_r$ . For small system sizes,  $t_m$  and  $t_r$  are of the order of  $10^3$ , but for our largest systems ( $L \simeq 10^4$ ) we used  $t_r \geq 5 \times 10^6$  and  $t_m = 2.5 \times 10^6$ . We verified that our results show no systematic variation with time for  $t > t_r$ . A run consists of  $N_s$  independent trials, each with a different initial configuration, with  $N_s$  ranging from  $2 \times 10^5$  for L = 100, to 500 or 1000 for  $L \simeq 10^4$ . In practice  $t_m$  is limited because for  $\zeta \simeq \zeta_c$ , the survival probability decays sensibly over this time scale; in some cases only about 25% of the trials survive to time  $t_r + t_m$ .

Fig. 1 shows the overall dependence of the stationary active-site density as a function of  $\zeta$ ; the points represent extrapolations of results for L = 100 - 5000 to the  $L \to \infty$  limit. The data indicate a continuous transition from an absorbing state ( $\rho_a = 0$ ) to an active one at  $\zeta_c$  in the vicinity of 0.95.

Our first task is to locate the critical value  $\zeta_c$ . We studied the stationary active-site density,  $\rho_a$ , and its second moment  $\rho_a^2$ , anticipating that as in other absorbing-state phase

transitions, the active-site density (i.e., the order parameter) will obey finite-size scaling [23]:

$$\overline{\rho_a}(\Delta, L) = L^{-\beta/\nu_\perp} \mathcal{R}(L^{1/\nu_\perp} \Delta) , \qquad (3)$$

where  $\Delta \equiv \zeta - \zeta_c$ , and  $\mathcal{R}$  is a scaling function with  $\mathcal{R}(x) \sim x^{\beta}$  for large x, since for  $L \gg \xi \sim \Delta^{-\nu_{\perp}}$  we expect  $\overline{\rho_a} \sim \Delta^{\beta}$  (here  $\xi$  is the correlation length). When  $\Delta = 0$  we have that  $\overline{\rho_a}(0,L) \sim L^{-\beta/\nu_{\perp}}$ . For  $\Delta > 0$ , by contrast,  $\overline{\rho_a}$  approaches a stationary value, while for  $\Delta < 0$  it falls off as  $L^{-d}$ . Thus in a double-logarithmic plot of  $\overline{\rho_a}$  versus L (see Fig. 2), supercritical values ( $\Delta > 0$ ) are characterized by an upward curvature, while for  $\Delta < 0$  the graph curves downward. Using this criterion (specifically, zero curvature in the data for  $L \geq 1000$ ), we find  $\zeta_c = 0.94887(7)$ , with the uncertainty reflecting the scatter in our numerical results for the curvature (see Fig. 2, inset). The associated exponent ratio is  $\beta/\nu_{\perp} = 0.235(11)$ . A similar analysis of the data for  $\rho_a^2$  yields  $\zeta_c = 0.94883(5)$  with an exponent of  $2\beta/\nu_{\perp} = 0.483(18)$ . We therefore adopt the estimates  $\zeta_c = 0.94885(7)$  and  $\beta/\nu_{\perp} = 0.239(11)$ .

We measured the autocorrelation function for the number of active sites  $N_a$ ,

$$C(t) = \frac{\langle N_a(t_0 + t)N_a(t_0)\rangle - \langle N_a\rangle^2}{\langle N_a^2 \rangle - \langle N_a \rangle^2}$$
(4)

in the stationary state. To obtain clean results for C(t) we study surviving trials in relatively long runs (from  $t_m = 2 \times 10^5$  for L = 625, to  $5 \times 10^6$  for  $L = 10^4$ ; this obliges us to reduce our sample to 200 surviving trials for  $L \leq 2500$  and 100 surviving trials for  $L \geq 5000$ ). Results for  $\zeta = 0.9488$  are shown in Fig. 3: C(t) decreases monotonically, but does not follow a simple exponential decay. To study the dependence of the relaxation time on system size, we determine the temporal rescaling factor r required to obtain a data collapse between C(t; L/2) and C(t/r; L). A good collapse is possible (see Fig. 3), but the rescaling factor depends on L; for  $L = 2^n \cdot 625$ , we use  $t^* = t/r^n$  with r = 2.93, 2.91, and 2.89 for n = 1, 2, and 3, respectively. The rescaling factor r appears to approach a limiting  $(L \to \infty)$  value of 2.80(5), corresponding to a relaxation time that scales as  $\tau \sim L^{\nu_{\parallel}/\nu_{\perp}}$  with  $\nu_{\parallel}/\nu_{\perp} \equiv z = \ln r/\ln 2 = 1.49(3)$ . We also studied the half-life  $\tau_H$  (the time for the survival probability to decrease by a factor of 1/2 in the stationary state) at  $\zeta_c$ . This relaxation time exhibits a clean power-law dependence on system size,  $\tau_H \sim L^z$ , with z = 1.42(1).

Next we examine the stationary scaling of the order parameter away from the critical point. We determined the stationary active-site density  $\overline{\rho_a}(\zeta, L)$ , for  $\zeta$  in the vicinity of  $\zeta_c = 0.94885$ , and for system sizes L = 100 - 5000. We analyze these data using the finite-size scaling form of Eq. (3), which implies that a plot of  $L^{\beta/\nu_{\perp}}\overline{\rho_a}(\Delta, L)$  versus  $L^{1/\nu_{\perp}}\Delta$  should exhibit a data collapse. We shift each data set (in a log-log plot of  $L^{\beta/\nu_{\perp}}\rho_a$  versus  $L^{1/\nu_{\perp}}\Delta$ ), vertically by  $(\beta/\nu_{\perp}) \ln L$ , using  $\beta/\nu_{\perp} = 0.239$  as found above, and determine the horizontal shift S(L) required for data collapse. These are found to follow the relation  $S(L) = \nu_{\perp}^{-1} \ln L$ , with  $\nu_{\perp}^{-1} = 0.553(3)$ . That these values yield an excellent data collapse is evident from Fig. 4. The slope of the scaling plot (linear regression using the 25 points with  $\ln(L^{1/\nu_{\perp}}\Delta) > -0.5)$ , yields  $\beta = 0.410(4)$ . This is somewhat smaller than, but consistent with, the estimate  $\beta = 0.43(2)$  obtained by combining  $\nu_{\perp}^{-1} = 0.553(3)$  and  $\beta/\nu_{\perp} = 0.239(11)$ . We adopt  $\beta = 0.42(2)$  as our final estimate.

#### **B.** Interface Representation

Interface representations are useful for studying both sandpiles [17–20] and particle systems such as the contact process [30]. Using such a representation, the activity history of the sandpile can be described in terms of an equation of motion that is an exact analog of a driven interface advancing in a quenched disordered medium. Our one-dimensional case is an example of a larger class of models, for which a mapping can be provided from the sandpile to an interface field [17–20]. Such a description can be useful, for example, in understanding the role of microscopic rules and in defining novel quantities for study.

The mapping is constructed as follows. Let the interface height variable  $H_i(t)$  count the number of topplings at site *i* up to time *t*. The dynamics of  $H_i(t)$  follows from the observation that the toppling of a site depends (through its height  $z_i$ ) on the number of particles it has received, and on the number of times it has toppled. Each time a neighbor of site *i* topples, site *i* gains one, two, or no particles, with probabilities of 1/2, 1/4 and 1/4, respectively. This allows a 'projection trick', in which the dynamics of  $H_i(t)$  is constructed from particle counting [20,12]. Topplings at the sites neighboring *i* give rise to an average incoming flux  $\bar{n}_i^{in}$  at site *i*, plus a fluctuating part  $\delta n_i^{in}$ , which records, in an exact manner, the random choices made for each particle. The average flux minus the number of topplings at *i* gives rise to a discrete Laplacian, while the fluctuating part can be mapped to a noise term  $\tau(i, H)$ , which can be evaluated for each toppling. Following these prescriptions, we find a discrete interface equation with quenched noise, which reproduces the sandpile activity [20]:

$$\frac{\partial H_i}{\partial t} = \Theta[\nabla^2 H_i + F_i - 1 + \tau(i, H)] \equiv \Theta(f_i)$$
(5)

where  $\Theta$  is the step function, so that  $H_i$  is nondecreasing. Since  $H_i(t)$  is restricted to integer values the time derivative should be interpreted as the rate of transitions from H to H + 1. The 'force'  $f_i$  at site *i* consists of the following contributions. The (discrete) Laplacian term arises, as noted above, from the balance between the average number of particles site *i* gains from, and loses to, its neighbors in toppling events. The 'columnar' noise term  $F_i$  represents the number of particles initially at site *i*, while  $\tau(i, H)$  is the fluctuation part of the particle flux associated with the *H*-th toppling of site *i*. The step-function character of the interface equation is discussed in greater detail in Ref. [20].

The noise-term  $\tau(i, H)$  is a quenched variable that arises from a mapping of the 'annealed' disorder of the original sandpile. Note that one could also consider the random choices of the particles' destinations at each toppling as a quenched, random landscape that is chosen in advance for each sandpile configuration. It is then easier to see that this maps into a quenched disorder term for the associated interface equation. This noise term is particle-conserving, and it has at each *i* a random-walk-like correlator  $\langle [\tau(H + \Delta H, i) - \tau(H, i)]^2 \rangle \sim \Delta H$ . If these correlations could be neglected, the scaling of the interface would follow that of the linear interface model in a quenched random field, as appears to be the case in two-and three-dimensional systems [12]. One should note, however, that long range-correlations in the noise can change the universality class, as has been shown numerically for another interface model [31]. The possible LIM universality classes are still under debate [32].

In the interface description the model undergoes a depinning transition at the critical force  $F_c \equiv \zeta_c$  [24,25]. At this point power-law correlations develop in the history of top-

plings. The interface behavior, assuming simple scaling, is described by two exponents: the roughness exponent  $\alpha$ , and the early-time exponent  $\beta_W$ . Introducing the width W as usual,

$$W^{2}(t,L) = \left\langle [H_{i}(t) - \bar{H}(t)]^{2} \right\rangle,$$
 (6)

(here  $\overline{H}(t)$  is the mean height), these exponents are defined via

$$W^{2}(t,L) \sim \begin{cases} t^{2\beta_{W}} & t \ll t_{\times} \\ L^{2\alpha} & t \gg t_{\times} \end{cases},$$
(7)

where the crossover time  $t_{\times} \sim L^z$ . Assuming that simple scaling holds and that the correlations in the interface can be described by a single length scale, we have the exponent relation  $\beta_W z = \alpha$ .

This scaling picture, familiar from the study of surface growth, was recently shown to apply in the case of a simple absorning-state phase transition [30]. For the one-dimensional Manna model the situation is complicated by several factors. First, the noise appearing in the interface description has two components,  $\tau(i, H)$  and  $F_i$ . The interface behavior will therefore exhibit a crossover from a regime dominated by the initial configuration (reflected in  $F_i$ ) to a randomness-dominated regime. This effect also appears in higher dimensions, but in d = 1, due to the meager phase space, relaxation is much slower and transient effects may be much more severe. Note that the *H*-independent terms on the r.h.s. of the interface equation can be understood as an initial height profile, which then relaxes to the asymptotic rough state [20]. It is easy to see that by varying such an initial condition different transients can be generated.

A problem with one-dimensional models is that the two-point correlation function of the surface roughness scales with a different exponent,  $\alpha_{loc}$ , which for fundamental reasons is limited to  $\alpha_{loc} \leq 1$ . The exponent  $\alpha$  can attain a larger value, for example  $\alpha = 1.25$  for the one-dimensional linear interface model [26]. These exponents are related via  $\alpha = \alpha_{loc} + \kappa$ , where  $\kappa$  measures the divergence of the height difference between neighboring sites with L. In the corresponding 1-d linear interface model, this is termed 'anomalous scaling' [26,27]. This means that as  $t \to \infty$ , the typical height difference between neighboring sites increases without limit. Since larger systems have a greater lifetime, this has implications for the roughness as measured by  $W_{sat}^2 \equiv \lim_{t \to t_c} W^2(t, L)$ , with  $t_c$  the time at which the absorbing state with no activity is reached, i.e., the lifetime. The saturation width  $W_{sat}$  scales as  $L^{\alpha}$ , with  $\alpha$  related to  $\beta_W$  and z as above. In models exhibiting an absorbing state, such as the contact process or a FES, the width saturates only because all activity eventually ceases; the width in *surviving* trials does not saturate. This is in marked contrast to the behavior of interface models, in which the width saturates due to the Laplacian term representing surface tension. (Continuum descriptions of absorbing-state phase transitions, and their associated interface representations, likewise include a Laplacian term, but the noise driving the interface grows without limit, so saturation is not required while there is activity [30].)

Finally, in absorbing-state models, interface scaling appears to be strongly linked to the approach to the stationary state. In a model with simple scaling (i.e., unique diverging length and time scales, and no conserved quantities), the growth exponent  $\beta_W$  is related to the critical exponent  $\theta$  governing the initial decay of activity via  $\beta_W + \theta = 1$  [30]. In the present case relaxation is complicated by effects that may mimic (for a certain time) columnar disorder, and slowly relaxing perturbations (the long-wavelength density fluctuations mentioned in Sec. II).

In simulations we first studied the time-dependent mean interface width  $W^2(t, L)$  in systems of size L = 1253, 2506, 5012, 10024, and 20048, at the critical point  $\zeta = 0.94892$ . The dependence of the saturation width on system system size yields  $\alpha = 1.42(1)$ . We may then attempt to collapse the data for  $W^2(t, L)$  using this exponent, and varying z to obtain the best collapse; in this way we find z = 1.65(2). The resulting scaling plot (Fig. 5), of  $\tilde{W}^2 \equiv W^2/L^{2\alpha}$  versus  $\tilde{t} \equiv t/L^z$ , shows a good collapse, and an apparent power-law growth in the roughness, following an initial transient. From the scaling relation  $\beta_W = \alpha/z$  we obtain  $\beta_W = 0.863(13)$ , while a direct fit to the time-dependent width data yields  $\beta_W = 0.87(2)$ .

For comparison, an independent series of studies at  $\zeta = 0.9490$  were performed to determine the lifetime  $t_c$  and saturation width  $W_c$  for L = 400 to L = 6400. Power-law fits to these data yield essentially consistent results, i.e.,  $\alpha = 1.48(2)$ ,  $\beta_W = 0.86(2)$  and z = 1.70(3). Fig. 6 shows a clear power-law dependence of the saturation width on the lifetime in *individual runs*. This indicates that a normal Family-Vicsek-style scaling plot of W(t, L) as in Fig. 5 is problematic, since as noted above the width in any surviving run does not saturate as would be the case in normal interface models, and the saturation width  $W \sim w_c$  will therefore depend on how long the particular configuration stays alive.

Similarly to the case of the linear interface model, we find that there is an independent local roughness exponent  $\alpha_{loc}$  that describes the two-point k-th order height-height correlation function  $G_k(r) = \left\langle |H_{i+r} - H_i|^k \right\rangle \sim r^{k\alpha_{loc}}$  for  $r < \xi(t) \sim t^{1/z}$ . We find  $\alpha_{loc} = 0.59(3)$ for  $k = 1 \dots 8$ . This shows that the interface is simply self-affine, not multifractal. We note, however, that the interface exponents of the Manna sandpile are not those of the one-dimensional LIM. This is most likely due to the fact that, perhaps differently from the two- and higher-dimensional cases, here it is important that the noise term *increases* in strength with the propagation of the interface, or with sustained activity. This arises from the fact that the fluctuations in the number of grains received at each site, reflected in  $\tau(H,i)$ , follow random-walk characteristics. Thus the anomaly exponent  $\kappa$  indicates an even stronger dependence of the step height on L at saturation than in the LIM. The same is also true if the step height is considered as a function of time for  $t < t_c$ . We find that  $\kappa_{Manna} \sim 0.82 \sim \kappa_{LIM} + 0.5$ . Due to this time- or height-dependence of  $\tau$  there is a direct coupling of  $t_c$  and  $w_c$  with the final average height,  $H_c$  (see Fig. 7). As discussed above, this result follows, in the interface picture, from the fact that the noise strength increases with time. In the LIM,  $t_c$  and  $w_c$  are not correlated on a sample-to-sample basis.

### C. Initial Relaxation

A comparison of our results for stationary correlations  $(z \simeq 1.45)$  with those for the interface  $(z \simeq 1.7)$  suggests that the relaxation to the steady state and relaxation of fluctuations within the stationary regime show distinct scaling properties. This is supported by our results for the relaxation of the active-site density. At the critical point of a simple absorbingstate model such as the contact process, the activity density  $\rho_a$  exhibits an initial power-law decay,  $\rho_a \sim t^{-\theta}$ , followed by a crossover to the quasi-stationary value  $\rho_a \sim L^{-\beta/\nu_{\perp}}$  [29]. As noted above the growth exponent is related to the activity-decay exponent via  $\theta + \beta_W = 1$ if only one timescale is present [30]. A plot of  $L^{\beta/\nu_{\perp}}\rho_a(t)$  versus  $t/L^z$  yields a data collapse to a scaling function that is independent of L. In the present case (Fig. 8), we see that the collapse is imperfect, and that the form of  $\rho_a(t)$  changes with L. Here z was chosen so as to optimize the collapse at long times, yielding z = 1.75(3). For large systems, the active-site density exhibits three distinct regimes before reaching the quasi-stationary state: an initial power-law decay (I), followed by a crossover to a slower power-law regime (II), and finally a rapid decay (III) to the stationary state. For L = 20048, the exponents associated with regimes I and II are 0.163 and 0.144, respectively. While the latter exponent is in reasonable agreement with the scaling relation  $\beta_W + \theta = 1$ , it is clear that relaxation to the stationary state is more complicated for the sandpile than for, say, the contact process, which presents a unique power-law regime. A qualitative explanation may be found in the interface representation: the initial dynamics is dominated by relaxation of the initial grain profile  $z_i$ , which in the interface language means that at short times the columnar noise,  $F_i$ , dominates.

Thus another facet of the relaxation process is the approach of the mean height to its global value,  $\zeta$ , at a site with initial height z(0). In Fig. 9 we plot the mean height  $\langle z(t)|z(0)\rangle$  in at system of 1400 sites at  $\zeta_c$ , averaged over 2000 trials. The inset shows that the asymptotic approach to  $\zeta$  is approximately power-law,  $|\langle z(t)|z(0)\rangle - \zeta| \sim t^{-\phi}$ , with  $\phi = \simeq 0.46, 0.45, 0.47, 0.50, \text{ and } 0.53$  for z(0) = 0, 1, 2, 3 and 4, respectively. All of these exponents are close to  $\phi = 1/2$ , the value expected for uncorrelated diffusion.

## D. Effects of initial preparation

In light of the complicated pattern of relaxation noted in the preceding subsection, it is well to recall that initial-decay studies of simple models such as the contact process employ a uniform, featureless initial configuration, far from the absorbing state. This is usually arranged by setting the the activity density to unity, an option that is not available in the present case, if we want to fix the particle density to its critical value  $\zeta_c$ . Since the height is a discrete variable, some local variations in density and activity are inevitable. All the results described up to now were obtained using the random deposition (RD) initial preparation described in Sec. II. In this subsection we report on studies using initial configurations in which the  $N = \zeta L$  particles are distributed so as to reduce density fluctuations. We again employ the sequence  $L = 2^n \cdot 1253$ ,  $N = 2^n \cdot 1189$  (n = 0, ..., 4) corresponding to  $\zeta = 0.94892$ .

One way of suppressing density fluctuations is via restricted random deposition (RRD): we divide the system into blocks, each consisting of 25 (or in some cases 26) sites, and depositing at random, within each block, a fixed number (24 or 25) of particles. In this way we generate a height distribution very similar to that of standard RD, but with virtually no density fluctuations on scales > 50 sites. Our conclusions from RRD simulations are as follows. First, the stationary activity density is identical, to within uncertainty, to that found previously. Thus we may continue to use  $\beta/\nu_{\perp} = 0.239$  in the scaling analysis. Figure 10, a scaling plot of the activity density (as in Fig. 8), shows a reasonable data collapse at long times, whereas the initial phase does not collapse. (It does collapse in an unrescaled plot, showing that the early stage is a size-independent, presumably purely local process.) Once again z has been chosen to optimize the collapse at long times, which in this case gives z = 1.47(6). The final approach to the stationary state appears to follow a power law,  $\rho_a \sim t^{-\theta}$ , with  $\theta = 0.16(1)$ . Analysis of the interface representation yields z = 1.57(3),  $\alpha = 1.13(2)$  and  $\beta_W = 0.77(3)$ , consistent with the scaling relation  $\beta_W = \alpha/z$ . (The growth of the survival time with L suggests yet another value,  $z \simeq 1.3$ .) Thus for RRD, all of the exponents describing transient properties are different from those found in RD studies. The exponent z has decreased to a value consistent with stationary relaxation, perhaps due to suppression of slowly relaxing, long-wavelength density variations. The sum  $\theta + \beta_W$ , however, is now somewhat smaller than unity.

A second kind of initial configuration with reduced density fluctuations may be termed maximum activity (MA). In this case all sites are either empty or have height 2 (except for a single site, in case N is odd), and the spacing between sites with z = 2 is fixed at 1 or 2 sites, in a regular pattern, so the average density is constant on a scale of 50 or so sites. While the density is again uniform on large scales, the number of active sites is as large as possible (as in usual initial-decay studies), and consequently the height distribution is quite different from that in the RD or RRD configurations. For MA IC's we find  $\alpha = 1.12(4)$ ,  $\beta_W = 0.78(1)$ , and  $\theta = 0.168(6)$ . From the collapse of  $\rho_a(t)$  and of  $W^2(t)$ , we obtain, respectively, z = 1.47(4)and z = 1.49(2), while the survival time data again yield  $z \simeq 1.3$ . Thus our results for the two kinds of initial conditions, RRD and MA, with suppressed density fluctuations are in good agreement. This suggests that the precise form of the initial height distribution does not affect asymptotic scaling behavior.

A general conclusion from these studies is that suppressing density fluctuations reduces the apparent value of the exponent z, suggesting that the unusually slow relaxation observed using random deposition initial conditions is due to long-wavelength density variations. The exponents  $\alpha$  and  $\beta_W$  decrease as well, indicating that such density variations also provide a source of roughness for the interface dynamics. Further studies are required to determine whether the interface-growth exponents reported here are typical of an entire class of initial conditions (i.e., with reduced density fluctuations), or if their values may depend on other details of the initial preparation. Until such studies are performed, we cannot be sure that the exponents describing roughness and initial relaxation are well defined, describing asymptotic evolution, or merely represent apparent power laws over some limited range of times and system sizes. In none of the cases studied do we observe the simple initial relaxation of  $\rho_a$  typical of the contact process. This may be due to the impossibility of preparing a completely uniform, high-activity initial state, and/or to the conservation of particles.

## E. Ergodicity

In a recent study we found strong nonergodic effects in the BTW sandpile [12]. Given the randomness in the Manna sandpile rules, we do not expect such effects here. To test this hypothesis we plot (see Fig. 11) the active-site density  $\rho_a$  versus time in four individual trials in a system of 1000 sites near  $\zeta_c$ . The curves for  $\rho_a$  in the various trials are completely intermixed; their ranges of fluctuation about a common mean are roughly equal. This is in complete contrast to the BTW case, where a similar plot shows distinct mean values, and very different ranges of variation of  $\rho_a$ , in each trial [12]. Thus the Manna sandpile appears to be ergodic, in the sense that a time-average of  $\rho_a$  in a single realization is independent of the initial condition (after a short transient), and yields the same value as the stationary average of  $\rho_a$  over many trials. Nonergodicity in the BTW model has been associated with "hidden" conservation laws, i.e., a memory of the initial configuration that persists over the entire trial. The Manna sandpile seems to be free of such conservation laws: while we can not rigorously exclude their presence, their effect must in any event be much weaker than in the BTW case. This is of course consistent with the fact that the BTW dynamics is deterministic, while the redistribution of particles is stochastic in the present case. (As a simple example of this, recall that a nearest-neighbor pair with both sites empty (z = 0) is forbidden in the stationary state of the BTW sandpile, whereas no such restriction exists for stochastic toppling rules.)

## **IV. DISCUSSION**

We studied the scaling behavior of a one-dimensional fixed-energy sandpile with the same local dynamics as the Manna model. The model exhibits a continuous phase transition between an absorbing state and an active one at a critical particle density  $\zeta_c = 0.94885(7)$ . In the interface (integrated activity) picture this translates into a depinning transition with a fixed force (fixed-energy model) or a force that is ramped up at an infinitesimal rate (driven case) [19].

The phase transition in the one-dimensional stochastic sandpile is characterized by the critical exponents  $\beta = 0.42(2)$  and  $\nu_{\perp} = 1.81(1)$ , which differ significantly from those associated with directed percolation ( $\beta = 0.2765$ ,  $\nu_{\perp} = 1.0968$ ) and linear-interface depinning ( $\beta = 0.25(3)$ ,  $\nu_{\perp} \simeq 1.3$ ). While absorbing-state phase transitions are expected to fall generically in the directed percolation universality class [37,38], it is reasonable to exempt the Manna model from this rule, due to local conservation of particles; this conservation law is expected to alter the universality class. In fact, studies of various models with the same local conservation law as the Manna sandpile, in dimensions d > 1, indicate a new, common universality class for models sharing this feature [12,21,22].

Studying the interface representation of the model, we obtain the roughness exponent  $\alpha = 1.48(2)$  and growth exponent  $\beta_W = 0.86(2)$ , which should be compared with  $\alpha = 1.33(1)$ ,  $\beta_W = 0.839(1)$  for DP and  $\alpha = 1.25(1)$ ,  $\beta_W = 0.88(2)$  for LIM. Study of the height-height correlation function yields the local roughness exponent  $\alpha_{loc} = 0.59(3)$ ; the corresponding DP value is 0.63(3) [30]. Changing the initial condition to suppress long-wavelength density fluctuations, we obtain  $\alpha = 1.13(2)$  and  $\beta_W = 0.77(2)$ , which again differ from the values associated with DP and LIM. Comparing these results with the apparent agreement of the Manna exponents with those of the LIM in two dimensions implies that either the rough numerical equivalence is fortuitous, or that the noise  $\tau$  in the interface equation has a fundamentally different structure depending on the dimension. It is worth remarking that the measured roughness exponent is rather close to  $\alpha = 3/2$ , which is the value one expects if only the columnar component of the noise is relevant [39]. The other exponents, however, seem to be far from the columnar disorder universality class (i.e.,  $\nu_{\perp} = 2$ , z = 2,  $\beta = 1$ ,  $\beta_w = 3/4$ ) [39].

In linear interface models, translational invariance of the noise can be used to derive the scaling relation  $(2 - \alpha)\nu_{\perp} = 1$  [40]. This relation does not appear to be verified by our numerical results. Notice that in the context of interface depinning z can be linked to the other exponents by a scaling relation [40] which reads  $z = \beta/\nu_{\perp} + \alpha$ . Inserting the values of  $\beta$ ,  $\nu_{\perp}$  and  $\alpha$  measured in simulations, we obtain z = 1.7, which is consistent with the exponent obtained analyzing the scaling of the width, for RD initial conditions. Our results for initial conditions with reduced fluctuations do not, however, follow this scaling relation.

Understanding this in the interface picture by considering the height-dependent quenched noise term is a challenge.

Our results for the dynamic exponent z are conflicting. We have studied various definitions of the relaxation or correlation time: that for the decay of the activity autocorrelation in the stationary state (yielding z = 1.49(3)), one associated with the survival time  $(z = 1.42(1) \text{ for RD initial conditions, } z \simeq 1.3 \text{ for RRD and MA IC's})$ , and those associated with the surface roughness and the decay of activity (z = 1.70(5) for RD IC's, z = 1.52(5) for initial configurations with suppressed density fluctuations). At a simple absorbing-state phase transition, all of these relaxation times are of course governed by the same exponent. Whether the unusually large z associated with time-dependent behavior using random deposition derives, as we have suggested, from slow relaxation of long-wavelength density fluctuations in the initial configuration, is a subject for further investigation. Our studies of modified initial states support this notion, but to reach a definitive conclusion other classes of initial conditions will need to be examined. Indeed, we have noted that, given their apparent dependence on the initial state, it is not clear whether the exponents <math>z,  $\alpha$ ,  $\beta_W$  and  $\theta$  are well defined, i.e., whether the asymptotic behavior follows simple power laws.

We note that the present model does not exhibit the strong nonergodic effects observed in the fixed-energy version of the BTW sandpile. The relaxation of the mean height  $\langle z_i(t) \rangle$  from its initial value to the average,  $\zeta$ , follows a power law with an exponent  $\approx 1/2$ . We find good evidence for finite-size scaling, in contrast with most driven sandpiles [34–36]. In summary, we have identified a one-dimensional sandpile model that exhibits an absorbing-state phase transition as the relevant temperature-like parameter (the energy density) is varied. It appears to be the "minimal model" for absorbing-state phase transitions belonging to a new universality class associated with a conserved density. Preliminary studies indicate that the driven version of the model exhibits scale-invariant avalanche statistics [3,41]. We may therefore hope that analysis of the driven model, and of spreading of activity at the critical point of the fixed-energy system, will permit us to establish detailed connections between scale invariance under driving and the underlying absorbing-state phase transition.

Let us finally stress that while in higher dimensions the linear interface universality class and that of systems with absorbing states in the presence of a conserved static field seem to coincide, the results of this paper show that this equivalence appears to be broken in d = 1. It will be interesting to study other one-dimensional systems with absorbing states and an order parameter coupled to a static conserved field [4,21,22] in order to compare the critical exponents and anomalies with those reported in this paper.

#### Acknowledgments

We thank R. Pastor-Satorras and F. van Wijland for helpful comments and discussions. RD thanks CNPq for financial support and CAPES and FAPEMG for support of computer facilities. We acknowledge partial support from the European Network contract ERBFM-RXCT980183. MAM acknowledges support from the Spanish DGESIC project PB97-0842, and Junta de Andalucía project FQM-165.

# REFERENCES

- P. Bak, C. Tang, and K. Wiesenfeld, Phys. Rev. Lett. 59, 381 (1987); Phys. Rev. A 38, 364 (1988).
- [2] G. Grinstein, in Scale Invariance, Interfaces and Nonequilibrium Dynamics, NATO Advanced Study Institute, Series B: Physics, vol. 344, A. McKane et al., Eds. (Plenum, New York, 1995).
- [3] R. Dickman, M. A. Muñoz, A. Vespignani, and S. Zapperi, Braz. J. Phys. 30, 27 (2000).
   e-print: cond-mat/9910454.
- [4] M. A. Muñoz, R. Dickman, R. Pastor-Satorras, A. Vespignani, and S. Zapperi, "Sandpiles and absorbing state phase transitions: recent results and open problems," to appear in *Proceedings of the 6th Granada seminar on computational physics*, Ed. J. Marro and P. L. Garrido. (American Institute of Physics, 2001). e-print: cond-mat/0011447.
- [5] C. Tang and P. Bak, Phys. Rev. Lett. **60**, 2347 (1988).
- [6] A. Vespignani and S. Zapperi, Phys. Rev. Lett. 78, 4793 (1997); Phys. Rev. E 57, 6345 (1998).
- [7] R. Dickman, A. Vespignani, and S. Zapperi, Phys. Rev. E 57, 5095 (1998).
- [8] A. Vespignani, R. Dickman, M. A. Muñoz, and Stefano Zapperi, Phys. Rev. Lett. 81, 5676 (1998).
- [9] M. A. Muñoz, R. Dickman, A. Vespignani, and Stefano Zapperi, Phys. Rev. E 59, 6175 (1999).
- [10] A. Chessa, E. Marinari and A. Vespignani, Phys. Rev. Lett. 80, 4217 (1998).
- [11] A. Montakhab and J. M. Carlson, Phys. Rev. E 58, 5608 (1998).
- [12] A. Vespignani, R. Dickman, M. A. Muñoz, and S. Zapperi, Phys. Rev. E 62, 4564 (2000).
- [13] D. Dhar, Physica A **263**, 4 (1999), and references therein.
- [14] V. B. Priezzhev, J. Stat. Phys. **74**, 955 (1994); E. V. Ivashkevich, J. Phys. A **27**, 3643 (1994); E. V. Ivashkevich, D. V. Ktitarev and V. B. Priezzhev, Physica A **209**, 347 (1994).
- [15] S. S. Manna, J. Phys. A **24**, L363 (1991).
- [16] S. S. Manna, J. Stat. Phys. **59**, 509 (1990).
- [17] O. Narayan and A. A. Middleton, Phys. Rev. B 49 244 (1994).
- [18] M. Paczuski and S. Boettcher, Phys. Rev. Lett. 77, 111 (1996).
- [19] K. B. Lauritsen and M. Alava, cond-mat/9903346.
- [20] M. Alava and K. B. Lauritsen, cond-mat/0002406, to be published in Europhys. Lett.
- [21] M. Rossi, R. Pastor-Satorras, and A. Vespignani, Phys. Rev. Lett. 85, 1803 (2000).
- [22] R. Pastor-Satorras and A. Vespignani, Phys. Rev. E 62, R5875 (2000).
- [23] M. E. Fisher, in Proceedings of the International Summer School 'Enrico Fermi', Course LI, (Academic Press, New York, 1971); M. E. Fisher and M. N. Barber, Phys. Rev. Lett. 28, 1516 (1972); Finite Size Scaling, Ed. J. Cardy, North-Holland (Amsterdam), 1988.
- [24] A. -L. Barabási and H. E. Stanley, Fractal Concepts in Surface Growth, (Cambridge University Press, Cambridge, 1995).
- [25] T. Halpin-Healy and Y.-C. Zhang, Phys. Rep. 254, 215 (1995).
- [26] H. Leschhorn, Physica A **195**, 324 (1993).
- [27] J.M. López, M.A. Rodriguez, and R. Cuerno, Phys. Rev. E 56, 3993 (1997); J. M. López, Phys. Rev. Lett. 83, 4594 (1999);

- [28] F. Family and T. Vicsek, J. Phys. A 18, L75 (1985).
- [29] J. Marro and R. Dickman, Nonequilibrium Phase Transitions in Lattice Models (Cambridge University Press, Cambridge, 1999).
- [30] R. Dickman and M. A. Muñoz, Phys. Rev. E 62, 7632 (2000).
- [31] J. Schmittbhul and J.-P. Villotte, Physica A, 270, 42 (1999).
- [32] P. Chauve. T. Giamarchi and P. Le Doussal, Phys. Rev. B 62, 6241 (2000).
- [33] J. Krug, Adv. Phys. 46, 139 (1997).
- [34] L. P. Kadanoff, S. R. Nagel, L. Wu and S. Zhou, Phys. Rev. A 39, 6524 (1989).
- [35] M. De Menech, A. L. Stella, and C. Tebaldi, Phys. Rev. E 58, R2677 (1998); C. Tebaldi,
   M. De Menech, and A. L. Stella, Phys. Rev. Lett. 83, 3952 (1999).
- [36] B. Drossel, Phys. Rev. E **61**, R2168 (2000).
- [37] H. K. Janssen, Z. Phys. 42, 141 (1981); *ibid.* 58, 311 (1985).
- [38] P. Grassberger, Z. Physik. B 47, 465 (1982).
- [39] G. Parisi and L. Pietronero, Europhys. Lett. 16, 321 (1991); Physica A 179, 16 (1991).
- [40] M. Kardar, Phys. Rep. **301**, 85 (1998).
- [41] R. Dickman, unpublished.

# FIGURE CAPTIONS

FIG. 1. Stationary active-site density versus energy density  $\zeta$ . The points represent extrapolations of data for L = 100 - 5000 to the  $L \to \infty$  limit.

FIG. 2. Stationary active-site density versus system size. From bottom to top,  $\zeta = 0.948$ , 0.94857, 0.94864, 0.94874, 0.9488, 0.94892, 0.949, and 0.95. The inset shows the curvature b of the log-log plot as a function of  $\zeta$ , for  $L \ge 1000$ . The straight line is a least-squares linear fit.

FIG. 3. Inset: stationary autocorrelation function C(t) versus t at  $\zeta = 0.9488$ , for (left to right) L = 625, 1250, 2500, 5000, and 10<sup>4</sup>. In the main graph the data are plotted versus a rescaled time  $t^*$  defined in the text.

FIG. 4. Scaling plot of the active-site density versus  $\Delta \equiv \zeta - \zeta_c$ . Symbols: +: L = 100; •: L = 200; ×: L = 500; o: L = 1000;  $\Box$ : L = 2000;  $\diamond$ : L = 5000.

FIG. 5. Scaling plot of  $\tilde{W}^2 \equiv W^2/L^{2\alpha}$  versus  $\tilde{t} \equiv t/L^z$ , for  $\zeta = 0.9489$ , using  $\alpha = 1.41$ , and z = 1.645(13). System sizes (top to bottom) L = 1253, 2506, 5012, 10024, and 20048.

FIG. 6. Scaling plot of saturation width versus lifetime in individual trials,  $\zeta=0.9490,$  L=400-6400.

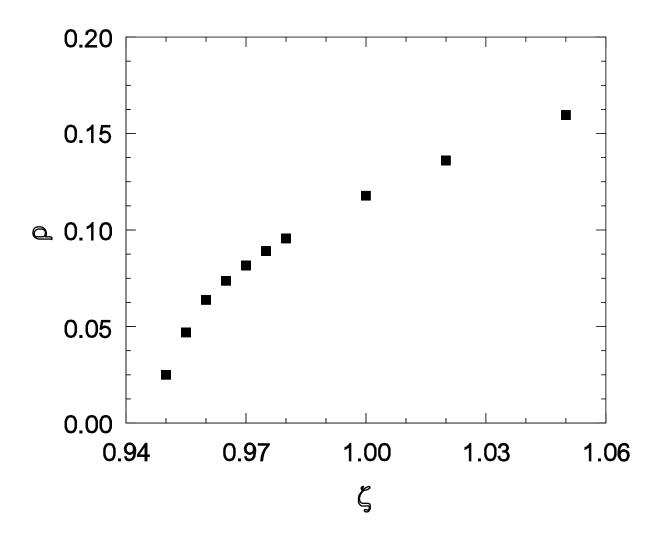
FIG. 7. Saturation height versus lifetime in individual trials,  $\zeta = 0.9490$ , L = 400-6400.

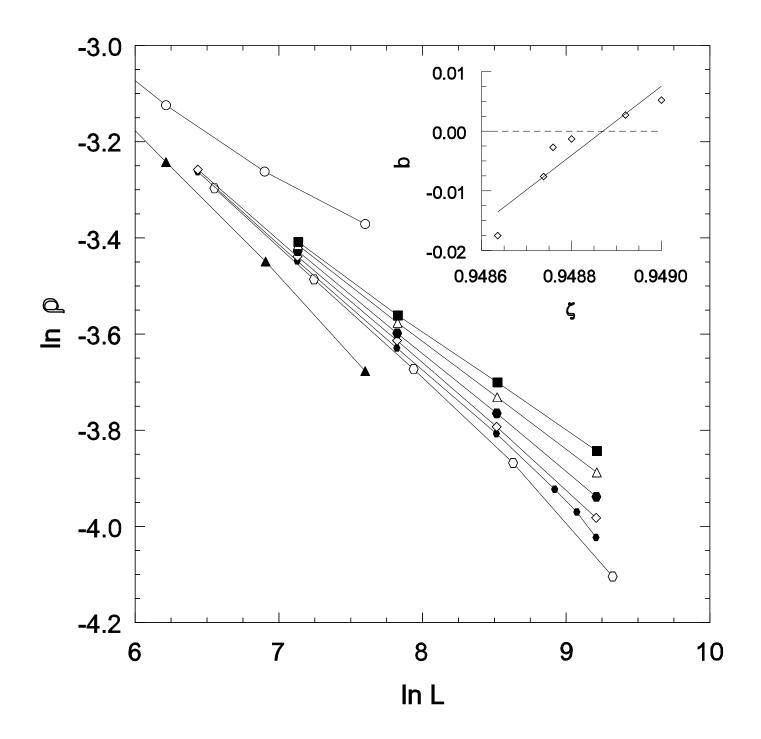
FIG. 8. Scaled active-site density  $\rho^* = L^{\beta/\nu_{\perp}}\rho_a$  versus scaled time  $t^* = t/L^z$  for  $\zeta = 0.9489$ , system sizes L = 1253,..., 20048 as indicated.

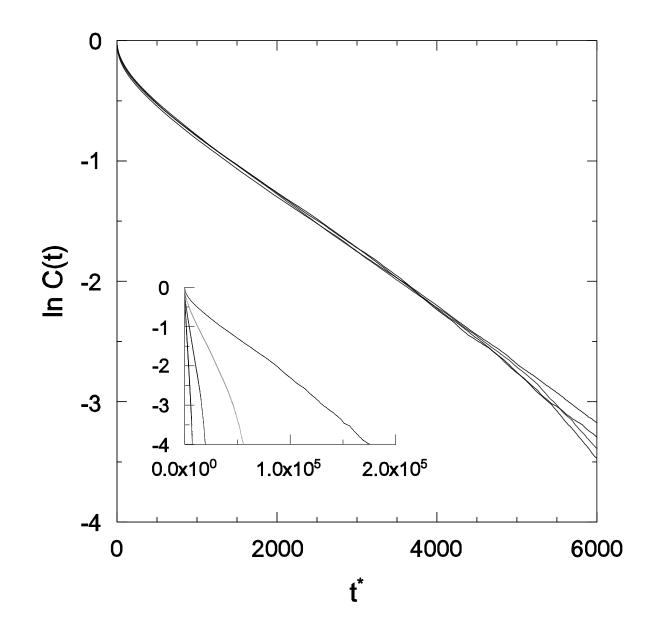
FIG. 9. Mean height  $\langle z(t)|z(0)\rangle$  of sites with initial height z(0), in at system of 1400 sites at  $\zeta_c$ , averaged over 2000 trials. From bottom to top: z(0) = 0, 1, 2, 3, and 4. The inset is a plot of  $\ln |\langle z(t)|z(0)\rangle - \zeta|$  versus  $\ln t$ .

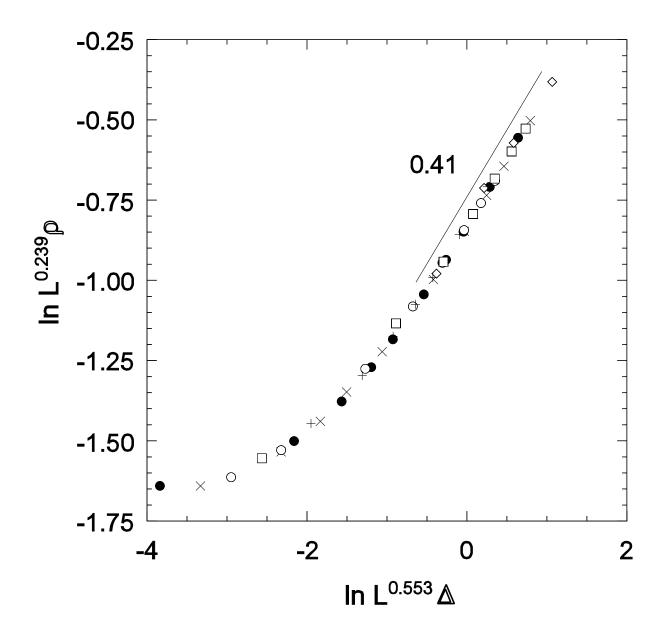
FIG. 10. Scaled active-site density versus scaled time for  $\zeta = 0.9489$  as in Fig. 8, but for RRD initial conditions.

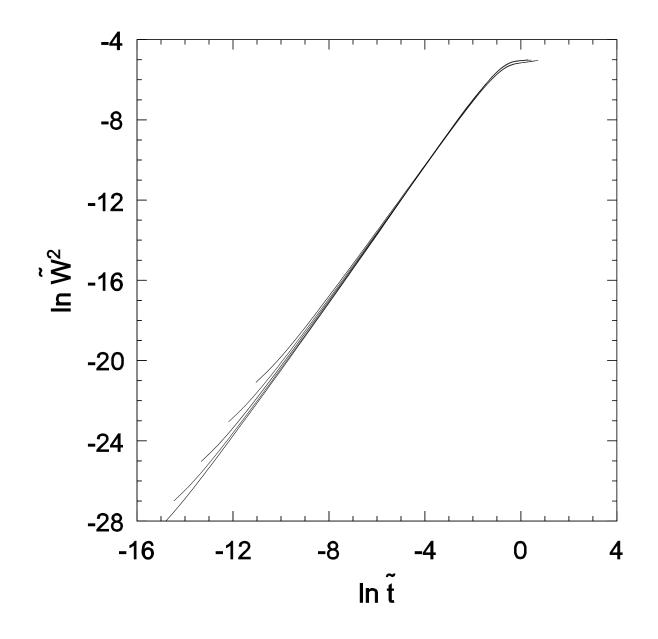
FIG. 11. Active-site density  $\rho_a(t)$  in four different trials at  $\zeta = 0.95$  in a system of 1000 sites.

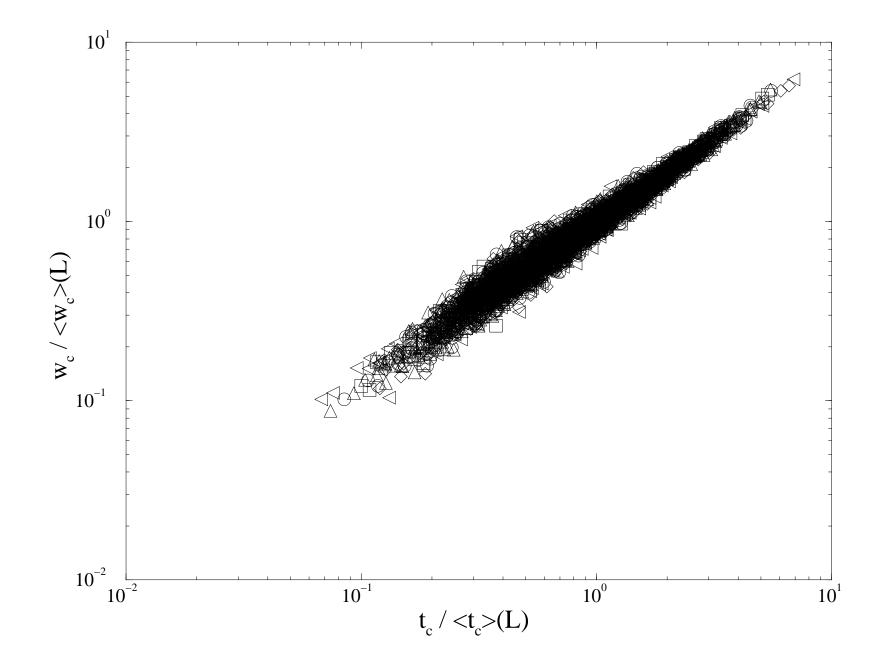


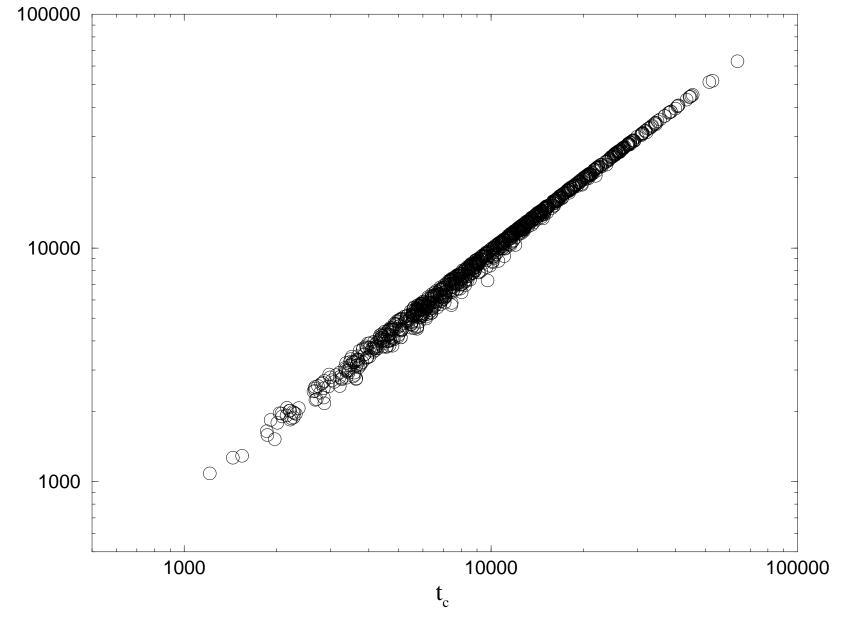












 $\overset{\mathrm{o}}{\mathrm{h}}$ 

